



## **A NUMERICAL ANALYSIS OF THE ELECTRICAL OUTPUT RESPONSE OF A NONLINEAR PIEZOELECTRIC OSCILLATOR SUBJECTED TO A HARMONIC AND RANDOM EXCITATION**

**Tiago Leite Pereira**

**Aline Souza de Paula**

**Adriano Todorovic Fabro**

tiagolei.tl@gmail.com

alinedepaula@unb.br

fabro@unb.br

Universidade de Brasília, Department of Mechanical Engineering

70.910.900 - Brasília – DF, Brazil

**Marcelo Amorim Savi**

savi@ufrj.br

Universidade Federal do Rio de Janeiro, COPPE , Department of Mechanical Engineering

21.941.972 – Rio de Janeiro – RJ, Brazil, P.O. Box 68.503

**Abstract.** *The renewable energy is in the focus of many researches in the last decades, and the use of piezoelectric material can be used to obtain one source of this renewable energy. In this case, energy harvesting explores mainly the source of ambient motion and the piezoelectric material convert mechanical energy, present in the ambient motion, into electrical energy. In the work, we present a nonlinear bistable piezomagnetoelastic structure subjected to harmonic and random base excitation. At first, harmonic excitation is of concern and then, the system subjected to random excitation is analyzed. The goal of the numerical analysis is to present an investigation of the best electrical output response of the system given harmonic and random excitations.*

**Keywords:** *Piezoelectric, nonlinear system, energy harvesting, random excitation*

## **1 INTRODUCTION**

Energy harvesting is a process where the available energy in the environment is converted into electrical energy. There are many sources of vibration energy and using piezoelectric material this kind of mechanical energy can be harvested by the piezoelectric direct effect, from which it can be used or stored. Recent works present significant contribution of the researches in energy harvesting (Anton and Sodano, 2007; Tang et al., 2010). In linear systems the best energy harvesting performance is achieved when the system is excited at its resonance frequency, if the excitation is slightly changed the electrical response of the systems is reduced. Nonlinearities allow a broader frequency band of excitation for optimal performance, enhancing the amount of harvested energy (Ramlan et al., 2009; Shahruz, 2007). Erturk (Erturk and Inman, 2008) presents a formulation of a cantilevered beam with piezoceramic layers and performance an analytical study of the energy harvested by the beam with a linear analysis. In a recent work (Erturk et al., 2009), considering a harmonic excitation, it was shown that the broadband behavior can be obtained by exploring nonlinearities of a bistable piezomagnetoelastic. Lefeuvre (Lefeuvre et al., 2007) were one of the first to investigate an energy harvesting system subjected to a random excitation. This same system was also studied by Kumar (Kumar et al., 2014), where a Gaussian white noise was considered and an investigation of the effects of the system parameters on the mean square voltage was studied. De Paula (De Paula et al., 2015) presented a numerically and experimentally investigation of the piezomagnetoelastic system when it is subjected to a Gaussian white noise and presented the influence of nonlinearities in the system. A comparison between the voltage provided from a linear, nonlinear bistable and nonlinear monostable systems was also investigated for De Paula, showing that for a bistable system the better RMS voltage is when the system visits both stable points. Therefore, this paper presents a numerical analysis aiming to compare the amount of energy harvested and to establish a methodology to compare the performance of the piezomagnetoelastic system. The methodology is based in the Power Spectral Density (*PSD*) of the input and the output response of the system when it is subjected to a harmonic and a random excitation. In section 1, a general introduction and general overview is presented. Section 2 presents the piezomagnetoelastic system and the main features of its dynamic behavior. Section 3 shows some numerical results and discussion considering, at first, harmonic and then random white noise excitation. Finally, in Section 4 some conclusion and final remarks are drawn.

## **2 PIEZOMAGNETOELASTIC STRUCTURE**

### **2.1 The Nonlinear System**

The energy harvesting system is based on a magnetoelastic structure first investigated by Moon and Holmes (Moon and Holmes, 1979), and Erturk (Erturk et al., 2009) describe the system as a structure that consists of a ferromagnetic cantilevered beam with two permanent magnets, one located in the free end of the beam and the other at a vertical distance  $d$  from the beam free end, subjected to harmonic and random base excitation. In order to use this device as a piezoelectric power generator, two piezoceramic layers are attached to the root of the cantilever and a bimorph generator is obtained as can be seen in Fig. 1

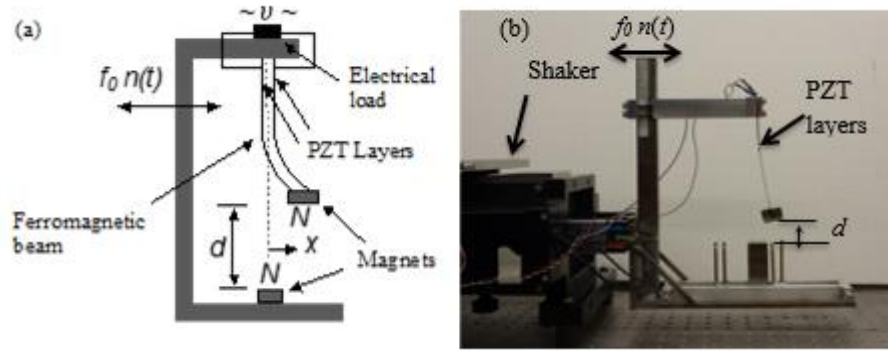


**Figure 1** (a) Schematic representation of the piezomagnetoelastic structure and (b) picture of the actual structure.

The system is governed by Eqs. (1) and (2)

$$\dot{x}' + 2\zeta\dot{x}' - \frac{1}{2}x(1-x^2) - \chi v = F(t), \quad (1)$$

$$v' + \lambda v + \kappa\dot{x} = 0, \quad (2)$$

where  $x$  is the dimensionless tip displacement of the beam in the transverse direction,  $v$  is the dimensionless voltage across the load resistance. The constant  $\zeta$  is the mechanical damping ratio,  $\chi$  is the dimensionless piezoelectric coupling term in the mechanical equation,  $\kappa$  is the dimensionless piezoelectric coupling term in the electrical circuit equation, and  $\lambda$  is the reciprocal of the dimensionless time constant ( $\lambda \propto 1/R_L C_p$  where  $R_L$  is the load resistance and  $C_p$  is the equivalent capacitance of the piezoceramic layers).  $F(t)$  is the forcing of the system, for a harmonic excitation  $F(t) = f_0 \cos(\omega t)$ , where  $f_0$  is the dimensionless excitation due to base acceleration ( $f_0 \propto \Omega^2 X_0$  where  $X_0$  is the dimensionless base displacement amplitude). And for a random excitation  $F(t) = N(\sigma, \bar{x})$ , where  $N(\sigma, \bar{x})$  is a Gaussian white noise with mean value  $\bar{x}$  and standard-deviation  $\sigma$ . The values of the parameters are considered as the same as in Erturk (Erturk et al., 2009):  $\zeta = 0.01$ ,  $\chi = 0.05$ ,  $\kappa = 0.5$ ,  $\lambda = 0.05$ . By considering these parameters, the equilibrium points, that are obtained from Eq. (1) and (2), are two stable spiral points located at  $(x, \dot{x}, v) = (\pm 1, 0, 0)$  and one instable saddle point located at  $(x, \dot{x}, v) = (0, 0, 0)$ .

## 2.2 Behavior when subjected to harmonic excitation

At first, the case of harmonic excitation is investigated. Figure 2 shows the qualitative change of system response from bifurcation diagrams by varying forcing parameters. In the diagram of Fig. 2 (a), the black points consider the system starting at  $\omega = 0.8$  and  $f_0 = 0.083$  with initial conditions  $(x, \dot{x}, v) = (1, 0, 0)$ , which corresponds to a chaotic response. Note that this behavior consists in a region in the middle of the bifurcation diagrams. From this chaotic response value of  $f_0$  is increased and decreased and plotted together in the diagram. The pink points present a similar analysis, however, the system is started at  $\omega = 0.8$  and  $f_0 = 0.083$  with initial condition  $(x, \dot{x}, v) = (1, 1, 0)$  which correspond to periodic orbit of periodicity 1. From this analysis, only periodic behavior is observed. In Fig. 2 (b), a similar analysis is evaluated, but now value of  $\omega$  is increased and decreased and once again plotted together in the bifurcation diagram. The black points consider the system starting at  $\omega = 0.8$  and  $f_0 = 0.1$  with initial conditions  $(x, \dot{x}, v) = (1, 0, 0)$ , and the pink point considers the system starting at  $\omega = 0.8$  and  $f_0 = 0.1$  with initial conditions  $(x, \dot{x}, v) = (1, 1, 0)$ . From

this analysis, the diagrams indicate periodic and chaotic behaviors. By considering black and pink points of both bifurcation diagrams, coexisting attractors are observed. In the following analysis, some of these responses are investigated.

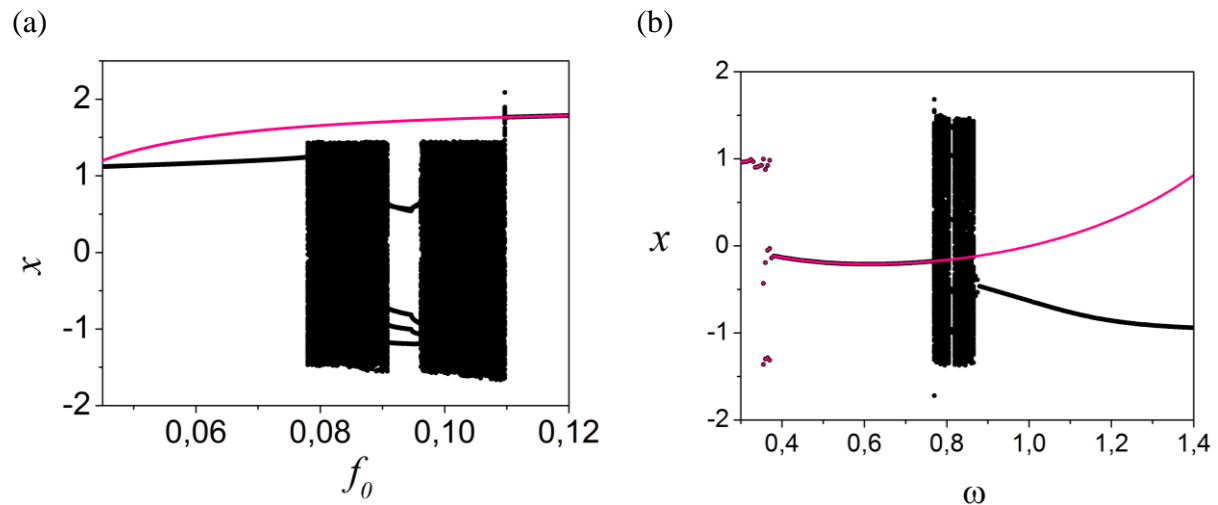


**Figure 2.** Bifurcation Diagram, (a) for  $\omega = 0.8$  and different values of  $f_0$  (b) and for  $f_0 = 0.1$  and different values of  $\omega$ .

From the bifurcation diagram presented in Fig. 2, different responses of the system can be seen. For the proposed analysis, 8 different cases of the response of the system, based on their behaviour identified from the bifurcation diagram, are chosen. Table 1 identifies all analysed cases. The cases are chosen in order to expose the different behavioural responses of the system. Table 1 also presents forcing parameters and initial conditions. Cases 1 to 3 are periodic with periodicity 1 and the phase space and Poincaré section are shown in Figure 3. Cases 4 to 6 are chaotic and the phase space and Poincaré section are presented in Figure 4(a)-(c). Cases 7 and 8 are periodic with periodicity 5 and the phase space and Poincaré section are shown in Figure 3.

For a better understanding of the behavior of the system, it can be observed that the cases 2 and 4 have the same forcing parameters but case 2 has a periodic response and case 4 has a chaotic response, this difference is related with different initials conditions, as can be seen in Table 1.

**Table 1.** Forcing parameters and initial condition

	$\omega$	$f_0$	Initial Condition	Behavior
Case 1	0.5000	0.1000	(1.4263, 0.4801, -0.7263)	Periodic
Case 2	0.8000	0.0830	(1.0000, 1.0000, 0.0000)	Periodic
Case 3	1.4000	0.1000	(0.9609, 2.966, -0.5192)	Periodic
Case 4	0.8000	0.0830	(1.0000, 0.0000, 0.0000)	Chaotic
Case 5	0.8000	0.1000	(-1.2316, -0.0048, 0.3478)	Chaotic
Case 6	0.8650	0.1000	(-0.6729, 0.2838, -0.1789)	Chaotic
Case 7	0.8000	0.0930	(-1.0000, 0.0000, 0.000)	Periodic
Case 8	0.8150	0.1000	(0.2983, 0.4198, -0.5181)	Periodic

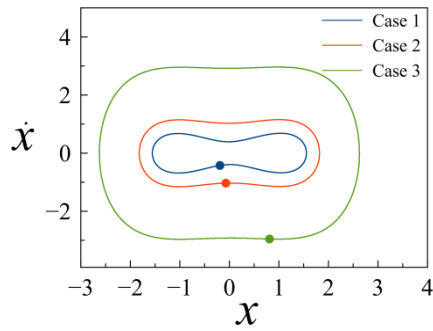


**Figure 3.** Phase space and Poincaré Section for case 1 to 3

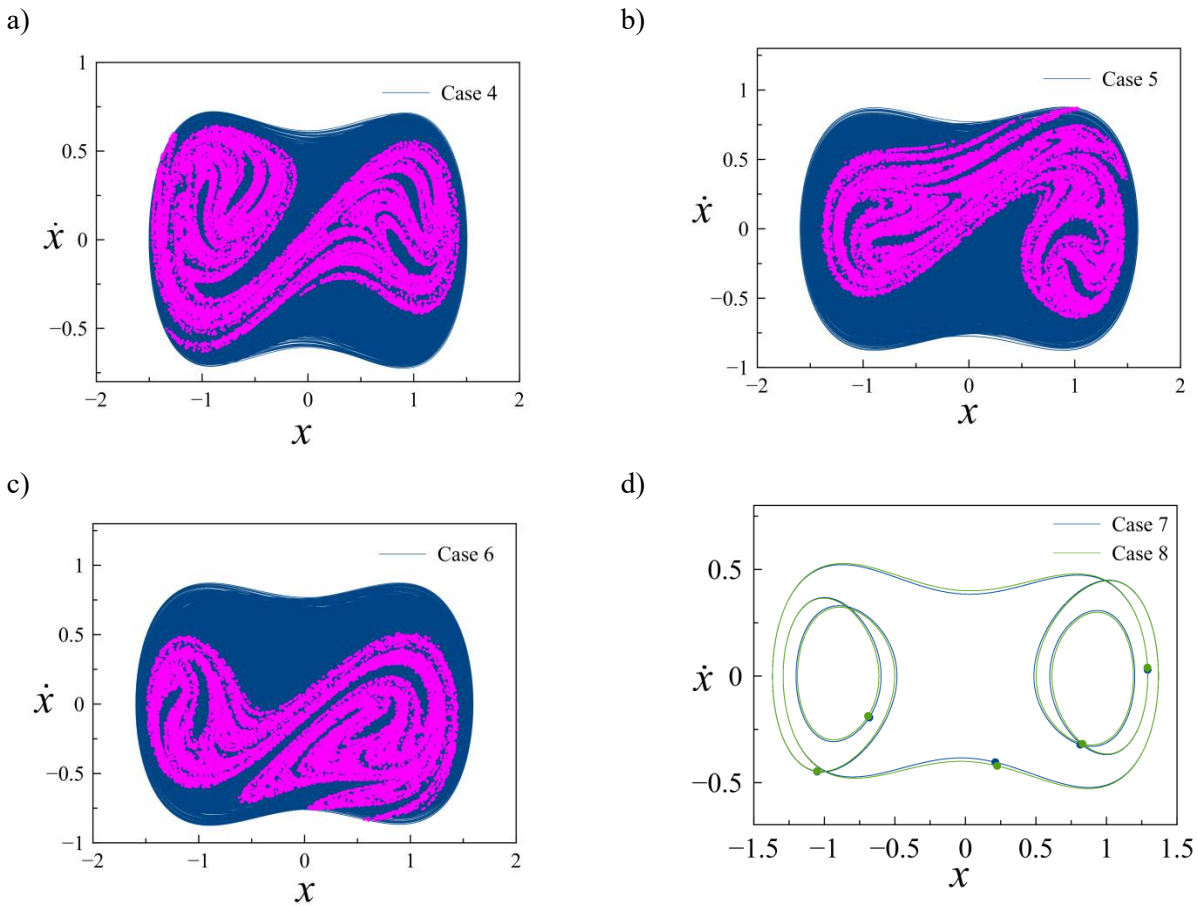


**Figure 4.** Phase space and Poincaré Section for (a) case 4, (b) 5, (c) 6 and (d) 7 and 8

### 3 PIEZOMAGNETOELASTIC STRUCTURE

This section is divided in two parts. The first is dedicated to the numerical simulations for the system subjected to a harmonic forcing, and the second to the Gaussian white noise forcing. To evaluate the system we propose the analysis based in the Power Spectral Density (PSD), that present the distribution of power into frequency domain.

$$\hat{x}(f) = \int_{-\infty}^{\infty} e^{-2\pi ift} x(t) dt \quad (3)$$

$$PSD = |\hat{x}(f)|^2 \quad (4)$$

where  $\hat{x}(f)$  is the Fourier Transform. The PSD of  $v(t)$  and  $F(t)$  are calculated using a periodogram approach and Hanning windowing (Newland, 2005). And area under the curve is estimated for both type of forcing and represents the Power of the Signal (PS). It is established the ratio of the  $PS_v$  and  $PS_f$  as a parameter to measure the performance of the system by:

$$r = \frac{\int_0^{\omega} PSD_v(\omega) d\omega}{\int_0^{\omega} PSD_f(\omega) d\omega} = \frac{PS_v}{PS_f}, \quad (5)$$

The bigger the value of the ratio  $r$ , the larger the area under the PSD of electrical response when compared to the mechanical input. Moreover, the value of  $PSD_v$  is related to electrical output. Thus,  $PS_v$  and  $r$  are parameters used to indicate system performance for different dynamical behaviour. The quantities  $v(t)$  and  $F(t)$  are dimensionless, so the  $PS_v$  and  $PS_f$  can be compared directly.

### **3.1 Harmonic Excitation**

The piezomagnetoelastic structure presents richness in the response when subjected to a harmonic forcing, as described in section 2. Three different of behavior in the response of the system are evaluated, periodic with periodicities 1 and 5 and chaotic, as it can be observed in Table 2. Figure 5 presents the response in time domain of cases 2, 4 and 7 and the spectrum of PSD, each one corresponding to one kind of evaluated behavior.

All cases, presented before in Table 1, are now assessed and Table 2 presents the kind of behavior of the system as well as the values for  $PS_v$ ,  $PS_f$  and its ratio  $r$ . It can be observed that cases 1 to 3 have similar periodic behavior but with different amplitudes. Although the  $PS_v$  are roughly in the same level of value, higher amplitudes are associated with higher values of  $PS_v$ , once the piezoelectric material is subjected to higher deformations. Case 3 presents the biggest  $PS_v$  between period-1 responses, therefore, the best electrical output and the best performance. According to the parameter  $r$ , the best performance in cases 1 to 3 is also case 3.

In cases 4 to 6 a chaotic response is presented, the best value for  $PS_v$  is presented in case 5 that also presents the best value of  $r$ . Cases 7 and 8 have a very similar response, as can be observed in Fig. 4 (d), therefore, the value of  $PS_v$  are very close as the piezoelectric material deformation is similar. However, the value of  $r$  is higher in case 7. Thus, case 7 has the best performance. This happens because of the value of the  $PS_f$ , case 7 and 8 have a similar behavior but the forcing parameters are different, which cause different value for the  $PS_f$ .

**Table 2.** Performance of the system subjected to a harmonic excitation for the eight cases under analysis.

	<i>Behavior</i>	$PS_f$	$PS_v$	$r$
Case 1	Periodic	0.3807	0.1056	0.2773
Case 2	Periodic	0.1639	0.1059	0.6461
Case 3	Periodic	0.1359	0.1336	0.9830
Case 4	Chaotic	0.6541	0.1711	0.2615
Case 5	Chaotic	0.9495	0.1953	0.2056
Case 6	Chaotic	0.8781	0.1634	0.1860
Case 7	Periodic	0.8212	0.2209	0.2689
Case 8	Periodic	0.9320	0.2198	0.2358

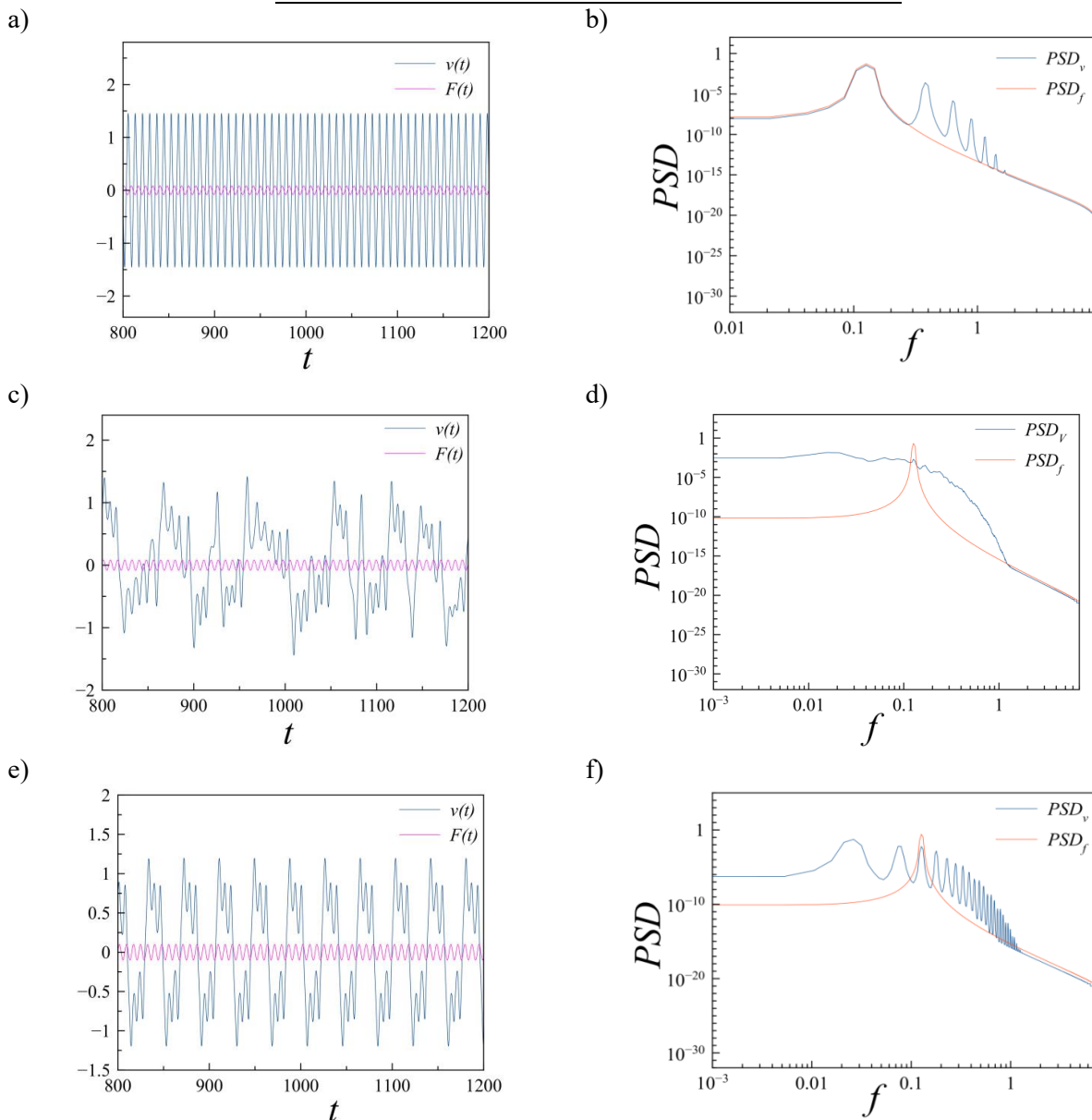


**Figure 5.** Response in time domain and the PSD curve for (a)-(b) case 2, (c)-(d) case 4 and (e)-(f) case 7

### 3.2 Harmonic Excitation

In this section, the systems performance is analysed under withe noise excitation. Ten different cases are presented and they are not related to the eight cases previously presented in harmonic excitation, i.e. they do not have the same dynamic behaviour necessarily. Cases were defined according to the random forcing parameter  $\sigma$ . Table 3 presents the value of forcing parameters. The response in time domain and the PSD spectrum is presented in Figure 6. In case 1 the system visits just one equilibrium point and in all the other cases the system visit both equilibrium points, as can be seen from the jumps in the time domain response of  $x(t)$ . It has been verified experimentally (De Paula et al., 2015) that when the system is subjected to a random vibration the bigger electric output is reached when the beam oscillates in both equilibrium points. This behaviour is also observed in Figure 6, that presents the excitation along with the electrical and mechanical responses. Both  $x(t)$  and  $v(t)$  are linearly related, as can be seen in Eqs. (1) e (2) , which implies that when the system vibrated in both equilibrium points, the electrical response is better.

It can be observed that the value of  $PS_f$  is increasing as the value of  $\sigma$  increases. A similar effect is observed in the value of  $PS_v$  however the value of  $r$  is best in case 3 when  $\sigma = 0.6$ . After case 5 starts to decrease. So the best case for a random white noise excitation is presented in case 3 that presents a good value for the  $PS_v$  and the best value for the parameter  $r$ . As the value of  $\sigma$  increases the PSD is spread out over frequency band under analysis, as can be verified from Figure 6. (b), (d) and (f).

**Table 3.** Performance of the system subjected to the 10 cases of random excitation.

	$\sigma$	$PS_f$	$PS_v$	$r$
<i>Case 1</i>	0.2	4.8393	0.0004	0.00008
<i>Case 2</i>	0.4	19.3575	0.0030	0.00015
<i>Case 3</i>	0.6	43.5544	0.0139	0.00031
<i>Case 4</i>	0.8	77.4301	0.0229	0.00029
<i>Case 5</i>	1.0	120.9845	0.0368	0.00030
<i>Case 6</i>	1.2	174.2178	0.0448	0.00025
<i>Case 7</i>	1.4	237.1297	0.0498	0.00021
<i>Case 8</i>	1.6	309.7205	0.0620	0.00020
<i>Case 9</i>	1.8	391.9900	0.0677	0.00017
<i>Case 10</i>	2.0	483.9383	0.0693	0.00014

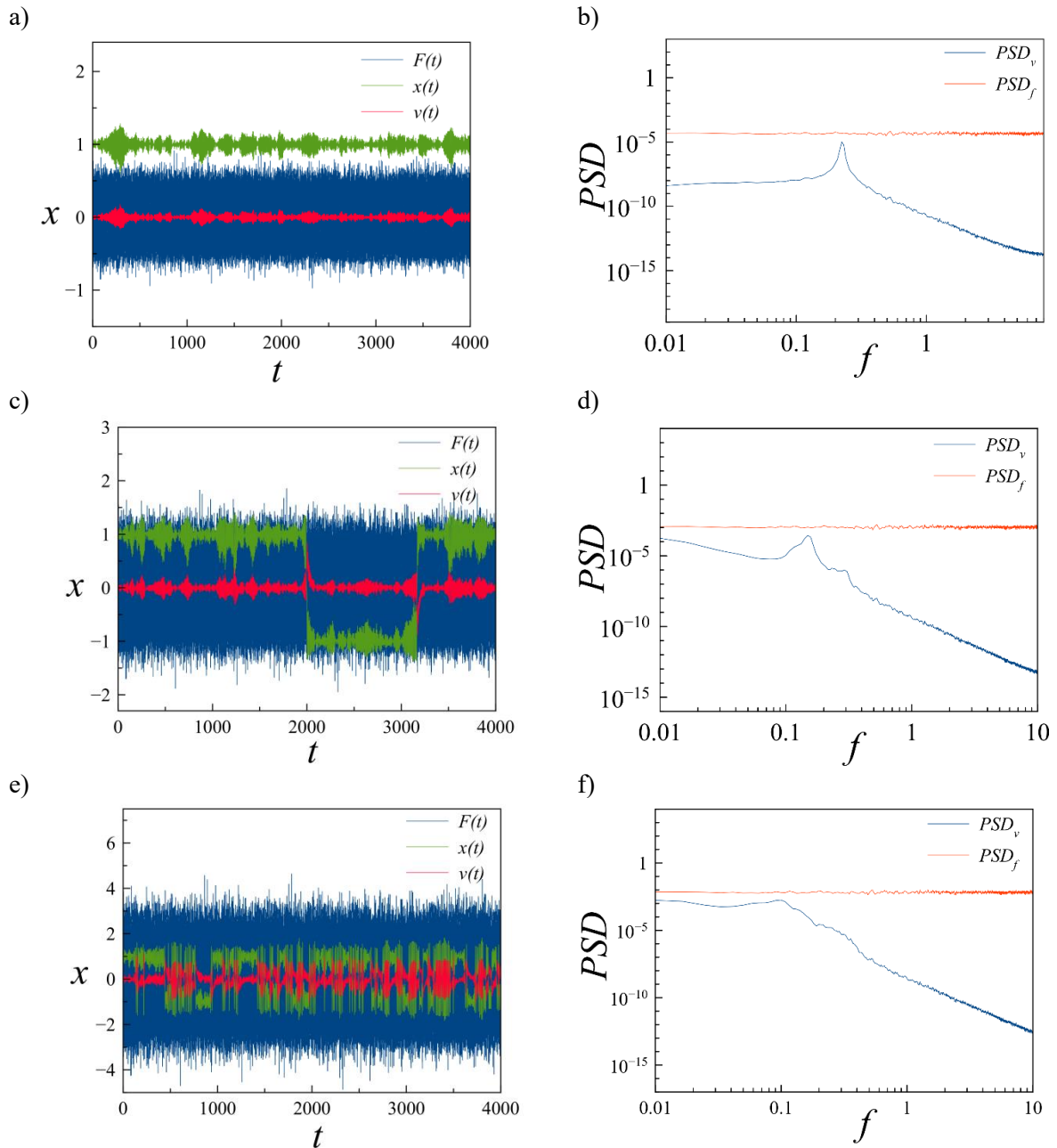


**Figure 6.** Response in time domain and the  $PSD$  curve for (a)-(b) case 1, (c)-(d) case 2 and (e)-(f) case 5.

## 4 CONCLUSION

In this work a non-linear model for a piezomagnetoelastic structure is presented. This system has a richness in the behavior of the response. For a harmonic excitation eight cases are chosen in order to verify the best performance, and the best case is presented when the system has very large amplitude in the periodic response. When the system has a chaotic response best performance is presented when the  $PS_f$  is the lowest. The same is stated when

the system present a periodic orbit of periodicity 5. When the system is subjected to a random excitation the best performance of the system increase until case 3, when the value of  $\sigma = 0.6$ , but the performance starts to decrease after case 5 when  $\sigma = 1.0$ . The ratio  $r$  of  $PS_v$  and  $PS_f$  is shown to be a good indicator for the performance of system for energy harvesting. For a future work a study of the system when the equation of motion is in the dimensionalized form can be simulated to a better understand of the value  $r$ .

## ACKNOWLEDGEMENTS

The authors would like to thank the Brazilian Research Agencies CNPq and CAPES for the support.

## REFERENCES

- Anton, S.R., and Sodano, H.A. (2007). A review of power harvesting using piezoelectric materials (2003?2006). *Smart Mater. Struct.* *16*, R1.
- De Paula, A.S., Inman, D.J., and Savi, M.A. (2015). Energy harvesting in a nonlinear piezomagnetoelastic beam subjected to random excitation. *Mech. Syst. Signal Process.* *54*, 405–416.
- Erturk, A., and Inman, D.J. (2008). A Distributed Parameter Electromechanical Model for Cantilevered Piezoelectric Energy Harvesters. *J. Vib. Acoust.* *130*, 041002–041002.
- Erturk, A., Hoffmann, J., and Inman, D.J. (2009). A piezomagnetoelastic structure for broadband vibration energy harvesting. *Appl. Phys. Lett.* *94*, 254102.
- Kumar, P., Narayanan, S., Adhikari, S., and Friswell, M.I. (2014). Fokker–Planck equation analysis of randomly excited nonlinear energy harvester. *J. Sound Vib.* *333*, 2040–2053.
- Lefeuvre, E., Badel, A., Richard, C., and Guyomar, D. (2007). Energy harvesting using piezoelectric materials: Case of random vibrations. *J. Electroceramics* *19*, 349–355.
- Moon, F.C., and Holmes, P.J. (1979). A magnetoelastic strange attractor. *J. Sound Vib.* *65*, 275–296.
- Newland, D.E. (2005). *An Introduction to Random Vibrations, Spectral & Wavelet Analysis: Third Edition* (Mineola, N.Y: Dover Publications).
- Ramlan, R., Brennan, M.J., Mace, B.R., and Kovacic, I. (2009). Potential benefits of a non-linear stiffness in an energy harvesting device. *Nonlinear Dyn.* *59*, 545–558.
- Shahruz, S.M. (2007). Increasing the Efficiency of Energy Scavengers. ArXiv07084412 Nlin.
- Tang, L., Yang, Y., and Soh, C.K. (2010). Toward Broadband Vibration-based Energy Harvesting. *J. Intell. Mater. Syst. Struct.* *21*, 1867–1897.